JOURNAL OF KUFA−PHYSICS
www.uokufa.edu.iq/journals/index.php/jkp | ISSN: 2077−5830

Estimating the lifetime and Reentry of the Aluminum Space Debris of Sizes (1 and 10 cm) in LEO under Atmosphere Drag Effects

*[1]H. K. Al-Zaidi [2]M. J. Al-Bermani [1]A.M. Taleb

*[1]*Department of Physics, College of Sciences, Baghdad University, Baghdad, Iraq*
[2]*Department of Computer Techniques Eng., University of Alkafeel, Alnajaf, Iraq*

*Corresponding Author E-mail: hamid_alzaidi@yahoo.com

ARTICLE INF

Article history:
Received: 31 MAR, 2020
Revised: 22 MAY, 2020
Accepted: 11 JUN, 2020
Available Online: 31 DEC, 2020

Keywords:

lifetime
Low earth orbit
space debris
Atmosphere Drag Effects

ABSTRACT

This study attempts to address the lifetime and reentry of the space debris in low earth orbit LEO which extends from 200 to 1200 km. In this study a new Computer programs were designed to simulate the orbit dynamics of space debris lifetime and reentry under atmospheric drag force using Runge-Kutta Method to solve the differential equations of drag force. This model was adapted with the Drag Thermosphere Model (DTM78, 94), the Aluminum 2024 space debris in certain size (1&10 cm) were used in this study, which is frequently employed in the structure of spacecraft and aerospace designs. The selected atmospheric model for this investigation was the drag thermospheric models DTM78 and DTM94, because of this dependence on solar and geomagnetic activities. It was found that the lifetime of the space debris increases with increasing perigee altitudes. It was also found that the elliptical shape of the debris orbit would change gradually into a circular shape, then its kinetic energy would be transformed into heat and hence the debris might be destroyed in the dense atmosphere.

DOI: http://dx.doi.org/10.31257/2018/JKP/2020/120207

تقدير عمر وزمن إعادة حطام الألمنيوم الفضائي للأحجام (١ و ١٠ سم) في المدار الأرضي المنخفض تحت تأثيرات سحب الغلاف الجوي

حامد كريم الزيدي ١* محمد جعفر البيرماني ٢ مهدي طالب رحمة الله ١

١ قسم الفيزياء-كلية العلوم-جامعة بغداد-بغداد- العراق
٢ قسم هندسة تقنيات الحاسوب- جامعة الكفيل- النجف الاشرف-العراق

الكلمات المفتاحية:

عمر الحطام
اعادة الحطام الفضائي
المدار الفضائي المنخفض
تأثير قوة سحب الغلاف الجوي

الـــخُـــلاصـــة

تسعى هذه الدراسة لمعالجة عمر وإعادة دخول الحطام الفضائي في المدار الأرضي المنخفض الذي يمتد من ٢٠٠ إلى ١٢٠٠ كم. حيث تم تصميم برامج حاسوبية جديدة لمحاكاة ديناميكيات المدار لعمر الحطام الفضائي وعودته تحت تأثير قوة سحب الغلاف الجوي باستخدام طريقة رانج-كوتا لحل المعادلات التفاضلية لقوة السحب. تم تكييف هذا النموذج مع نموذج سحب

الغلاف الجوي (DTM78, 94)، ، وتم استخدام الحطام الفضائي الألومنيوم ٢٠٢٤ في حجم معين (١ و ١٠ سم) في هذه الدراسة ، والتي يتم استخدامها غالبا في هيكل تصميمات المركبات الفضائية. نموذج الغلاف الجوي المحدد لهذا البحث هو نماذج السحب الحراري DTM78 و DTM94 ، بسبب أعتمادها على الأنشطة الشمسية والمغناطيسية الأرضية. وجد أن عمر الحطام الفضائي يزداد مع زيادة ارتفاعات الحضيض. وقد وجد أيضًا أن الشكل الإهليلجي لمدار الحطام يتغير تدريجيًا إلى شكل دائري ، ثم تتحول طاقته الحركية إلى حرارة وبالتالي يتم تدمير الحطام في الغلاف الجوي الكثيف.

1. INTRODUCTION

Johannes Kepler (1571-1630), studied the mass of observational data on the planet's positions collected by Tycho Brahe (1546-1601), formulated the three laws of planetary motion forever associated with his name. They know by Kepler's laws which are, in fact, a description of a special solution to the gravitational problem of n bodies [1]. Isaac Newton (1642-1727) was first realized and treated the problem systematically. Newton's laws of motion laid the foundation of the science of dynamics. They may be stated in the following form:

- Everybody continues in its state of rest or of uniform motion in a straight line except insofar as it is compelled to change that state by an external impressed force.

- The rate of change of momentum of the body is proportional to the impressed force and takes place in the direction in which the force acts, i.e. [2].

$$F \propto \frac{d(mv)}{dt} \qquad (a)$$

Thus, if the mass is constant,

$$F = m\frac{dv}{dt} \qquad (b)$$

Where F is the force, v is the velocity, and $\frac{dv}{dt}$ is the acceleration.

Newton evolved the law of gravitation between two particles as a result of his study of astronomy. His law of gravitation may be written as,

$$F = G\frac{Mm}{r^2}$$

1. Lifetime and Atmospheric Drag Theory and Experimental Methods

When the orbit perigee height is below 1000 km, the atmospheric drag effect becomes increasingly important [3]. Drag is a non-conservative force and will continuously take energy away from the orbit. Thus, the orbit semi major axis (a) and the period (T) are gradually decreasing the effect of drag [4]. The orbital velocity (v) is increasing. Atmospheric drag produces azimuthally deceleration that first reduces orbital ellipticity, then causes the debris particle to slowly spiral inwards towards the earth unit that rapidly rising density causes it to precipitously lose altitude and self-distract. The drag force is given by [5, 6].

$$F = \frac{1}{2m}C_D A\rho_a \, v^2 \qquad (1)$$

Where C_D the aerodynamic is drag coefficient, A is the average cross-section area of the debris and ρ_a is the air density. This force can be resolved into rectangular component, T is the tangential component, S is the radial component, and W is the normal component. Figure (1) shows these components [1,7].

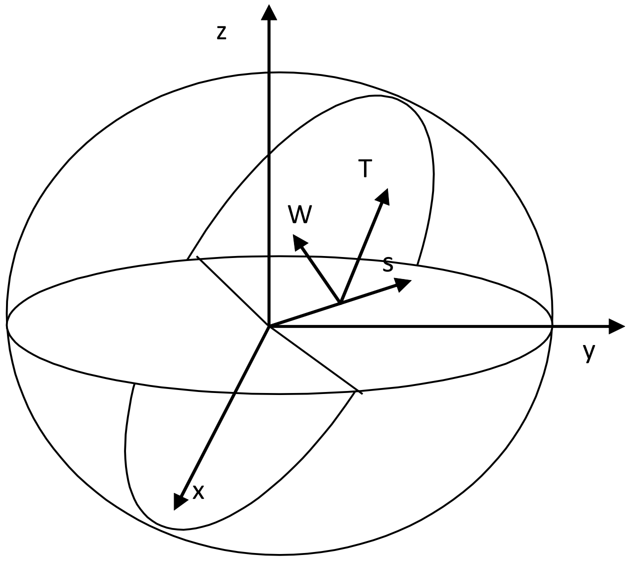

Fig.1: The components S, T, W [1]

Lagrange planetary differential equation of motion are used to determine the perturbed six elements under the effects of various disturbing function R^*, this function was originally expressed in terms of the elements a, e, I, Ω, ω, χ [1,8].

$$\frac{da}{dt}=\frac{2}{na}\frac{\partial R^*}{\partial e} \qquad (2a)$$

$$\frac{de}{dt}=-\frac{\sqrt{1-e^2}}{na^2e}\left(1-\sqrt{1-e^2}\right)\frac{\partial R^*}{\partial \varepsilon}-\frac{\sqrt{1-e^2}}{na^2e}\frac{\partial R^*}{\partial \omega} \qquad (2b)$$

A method due to Gauss enables this work to be short-circuited, obtaining the differential equations for the elements in terms of three mutually perpendicular components of the disturbing acceleration (S, T and W). To introduce S, T and W into the right-hand sides of the above equations we require expressions for $\frac{\partial R^*}{\partial \sigma}$ in terms of S, T and W, where σ is any element, it's found that:

$$\frac{\partial R^*}{\partial a}=\frac{r}{a}S \qquad (3a)$$

$$\frac{\partial R^*}{\partial e}=-aS\cos f+r\sin f\left(\frac{1}{1-e^2}+\frac{a}{r}\right)T \qquad (3b)$$

where f is the true anomaly, substituting these expressions into equations (2) we obtain,

$$\frac{da}{dt}=\frac{2}{n\sqrt{1-e^2}}\left(S\,e\sin f+\frac{pT}{r}\right) \qquad (4a)$$

$$\frac{de}{dt}=\frac{\sqrt{1-e^2}}{na}\left[S\sin f+T\left(\cos E+\cos f\right)\right] \qquad (4b)$$

Where E is the eccentric anomaly, p =a (1-e^2) and $E=\frac{\cos f+e}{1+e\cos f}$.

The drag force is in opposite direction to the debris or satellite motion, so that F=-T and normal component tends to zero (i.e. S=W=0), by substituting equation (1) into equations (4), the equations in terms of atmospheric drag are obtained.

$$\frac{da}{dt}=\frac{-A}{m}\frac{C_D\rho_a\,v^2}{n\left(1-e^2\right)^{\frac{1}{2}}}\left(1+e^2+2e\cos f\right)^{\frac{1}{2}} \qquad (5a)$$

$$\frac{de}{dt}=\frac{-A}{m}\frac{C_D\rho_a\,v^2}{na}\left(1-e^2\right)^{\frac{1}{2}}\frac{\cos f+1}{\left(1+e^2+2e\cos f\right)^{\frac{1}{2}}} \qquad (5b)$$

Where n is the mean motion, which equal to $\left(\frac{\mu}{a^3}\right)^{\frac{1}{2}}$, where μ is the gravitational constant. In order to obtain more reliable formulas, equations (5) can be transferred from the time dependent (t) to true anomaly (f) using the two body relationships.

$$r=\frac{a\left(1-e^2\right)}{1+e\cos f}, \quad r^2\dot{f}=h=\sqrt{\mu a(1-e^2)}, \quad n^2a^2=\mu,$$

$$\frac{dt}{df}=\frac{\left(1-e^2\right)^{\frac{3}{2}}}{n\left(1+e\cos f\right)^2}$$

And

$$v^2=\dot{r}^2+r^2\dot{f}^2=\frac{n^2a^2}{\left(1-e^2\right)}\left(1+e^2+2e\cos f\right) \qquad (6)$$

Therefore equation (5) becomes.

$$\frac{da}{df}=\frac{-A}{m}C_D\rho_a\,a^2\frac{\left(1+e^2+2e\cos f\right)^{\frac{3}{2}}}{\left(1+e\cos f\right)^2} \qquad (7a)$$

$$\frac{de}{df}=\frac{-A}{m}C_D\rho_a\,a\left(1-e^2\right)\frac{\left(1+e^2+2e\cos f\right)^{\frac{1}{2}}}{\left(1+e\cos f\right)^2}\left(\cos f+e\right) \qquad (7b)$$

To solve the equations in {a} and {e} it is useful to change the independent variable again, this time to the eccentric anomaly, using the relation.

$$\cos f = \frac{\cos E - e}{1 - e\cos E}$$

$$\sin f = \frac{\sqrt{1-e^2}\sin E}{1 - e\cos}$$

When these are done, we obtain [8].

$$\frac{da}{dE} = \frac{-A}{m} C_D \rho_a \, a^2 \frac{(1+e\cos E)^{\frac{3}{2}}}{(1-e\cos E)^{\frac{1}{2}}} \quad (8a)$$

$$\frac{de}{dE} = \frac{-A}{m} C_D \rho_a \, a \frac{(1+e\cos E)^{\frac{1}{2}}}{(1-e\cos E)^{\frac{1}{2}}} (1-e^2)\cos E \quad (8b)$$

From the above equations, we are determining the change in orbital parameters, and then the lifetime for space debris. The apogee and perigee distances are $[a(1+e)]$ *and* $[a(1-e)]$ respectively. When the changes in these over one revolution are computed using the derived relations.

$$\frac{dHa}{dE} = \frac{-A}{m} C_D \rho_a \, a(1+e) \frac{(1+e\cos E)^{\frac{1}{2}}}{(1-e\cos E)^{\frac{1}{2}}} (1+\cos E) \quad (9a)$$

$$\frac{dHp}{dE} = \frac{-A}{m} C_D \rho_a \, a^2(1-e) \frac{(1+e\cos E)^{\frac{1}{2}}}{(1-e\cos E)^{\frac{1}{2}}} (1-e\cos E) \quad (9b)$$

Runge-Kutta Method were used to solve the differential equations (9a & 9b), the formula for the Euler method is [9, 10],

$$y_{n+1} = y_n + hf(x_n, y_n) \quad (10)$$

Consider the use of a step like equation (10) to take a "trial" step to the midpoint of the interval. Then use the value of both x and y at that midpoint to compute the "real" step across the whole interval, in equations [9].

$$k_1 = hf(x_n, y_n)$$
$$k_2 = hf(x_n + \frac{1}{2}h,\ y_n + \frac{1}{2}k_1)$$
$$y_{n+1} = y_n + k_2 + O(h^3)$$

The above equations are called the second order Runge-Kutta or midpoint method. By far the most often used is the fourth order Runge-Kutta method. This method consists of the following four parameters.

$$k_1 = hf(x_n, y_n)$$
$$k_2 = hf(x_n + \frac{h}{2},\ y_n + \frac{k_1}{2})$$
$$k_3 = hf(x_n + \frac{h}{2},\ y_n + \frac{k_2}{2})$$
$$k_4 = hf(x_n + h,\ y_n + k_3)$$

The difference formula is given by.

$$y_{n+1} = y_n + \frac{k_1}{6} + \frac{k_2}{3} + \frac{k_3}{3} + \frac{k_4}{6} + O(h^5)$$

where h is the step size.

3. Results and Discussions

A computer program has been developed in this work to simulate the lifetime of space debris in orbit under the influence of atmosphere drag force. The numerical integration solved to equations (8), (9) by using Runge-Kutta method. The atmospheric model used is the DTM78,94 (drag thermosphere model) [11], that depends on solar and geomagnetic activities. The solar activity is represented by the solar flux index F10.7 at maximum activity 225. The geomagnetic activity is represented by the Kp Global index of values (0-9), the maximum value was taken (Kp=9).

In this work two spherical shape space debris made of aluminum (2024) density (2.785 gm/cm^3), diameters (1, 10 cm) [12,13] were selected for investigation. The selection criteria depend on the abundance of this type of aluminum in most spacecraft structures. The input parameters are shown in table (1).

Table 1: Aluminum debris (diameter =1, 10 cm) of reduction in semi major axis of the orbit parameters

Apogee altitude(km)	1200	1000	800	600	400	200
Perigee altitude(km)	500	500	500	400	200	150

Semi major axis(km)	7228	7128	7028	6878	6678	6553
Eccentricity	0.0484	0.035	0.0213	0.0145	0.0149	0.0038
Area/mass (cm^2/gm)	0.0717 &0.717	0.0717 &0.717	0.0717 &0.717	0.0717 &0.717	0.0717 &0.717	0.0717 &0.717

The outputs are shown in figures (2), (3), (4), (5). The change in semi major axis (a) were plotted against time (days) for different values of apogee and perigee altitudes. These results are applicable for space debris of size (1, 10 cm). It can be seen from these figures that the semi major axis values reduce to minimum until de-orbited. The calculated lifetime depends on apogee and perigee altitudes. The longest lifetime is 55 years at altitudes (1200-500 km) with diameter (10 cm). The shortest lifetime is 3 days at altitudes (200-150 km) with diameter (10 cm). Similarly, the lifetime of space debris of (1 cm) diameter is estimated. The longest lifetime is 11 years and the corresponding shortest is 0.5 day.

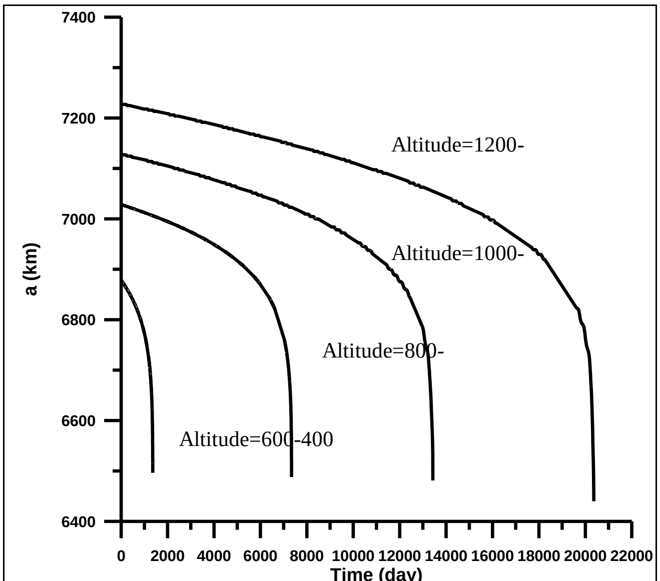

Fig.2: The behavior of semi major axis (a) with time of debris (diameter=10 cm).

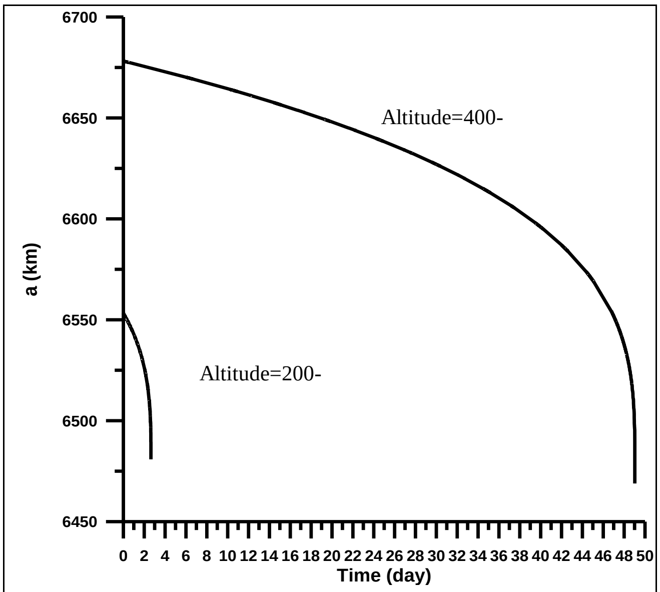

Fig.3: The behavior of semi major axis(a) with time of debris (diameter=10 cm).

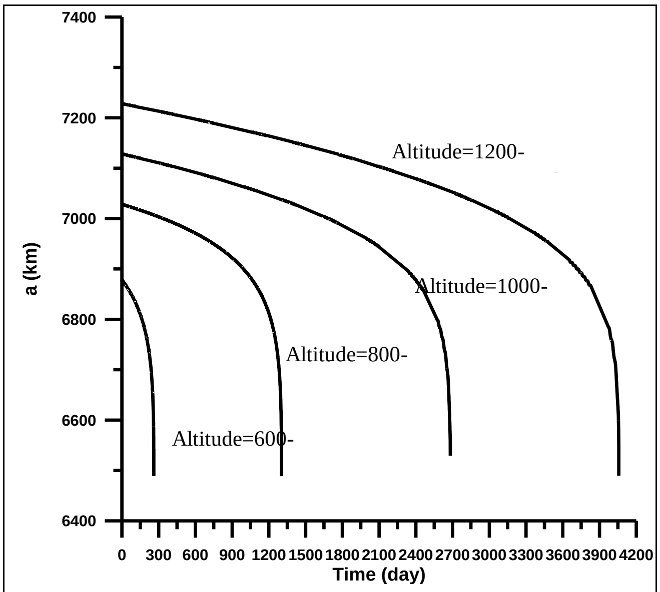

Fig.4: The behavior of semi major axis (a) with time of debris (diameter=1 cm).

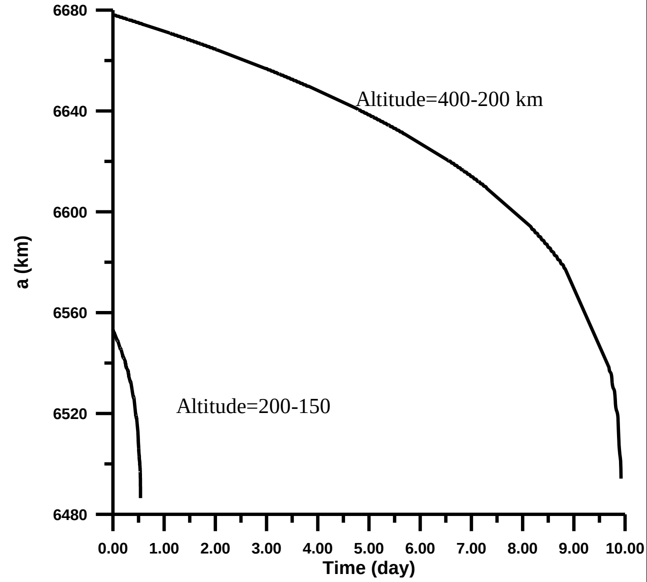

Fig.5: The behavior of semi major axis (a) with time of debris (diameter=1 cm).

The eccentricity (e) of the orbit was changed due to atmospheric drag force from elliptic to circular orbit until de-orbited in atmosphere. This behavior is illustrated in figures (6), (7), (8), (9). It can be seen from these figures that the eccentricity of the orbit decays slowly until de-orbited in the atmosphere.

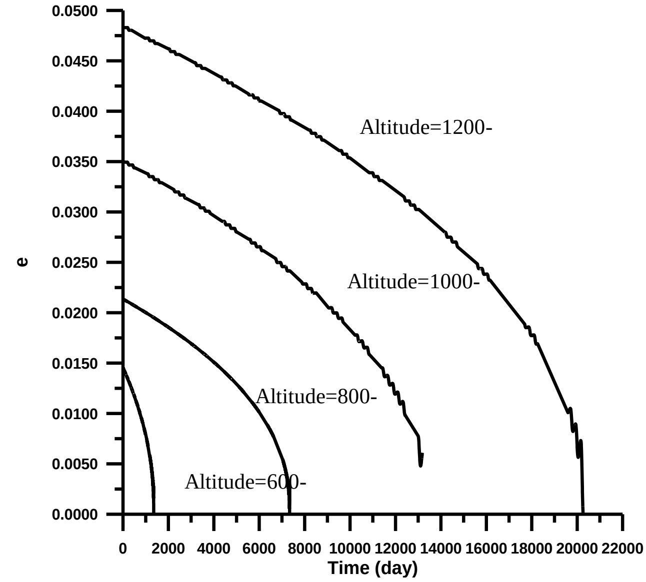

Fig.6: The behavior of eccentricity (e) with time of debris (diameter=10 cm).

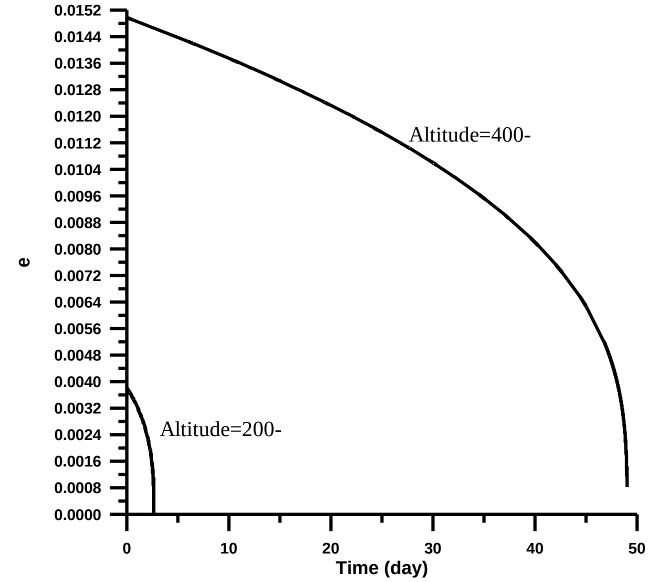

Fig.7: The behavior of eccentricity (e) with time of debris (diameter=10 cm).

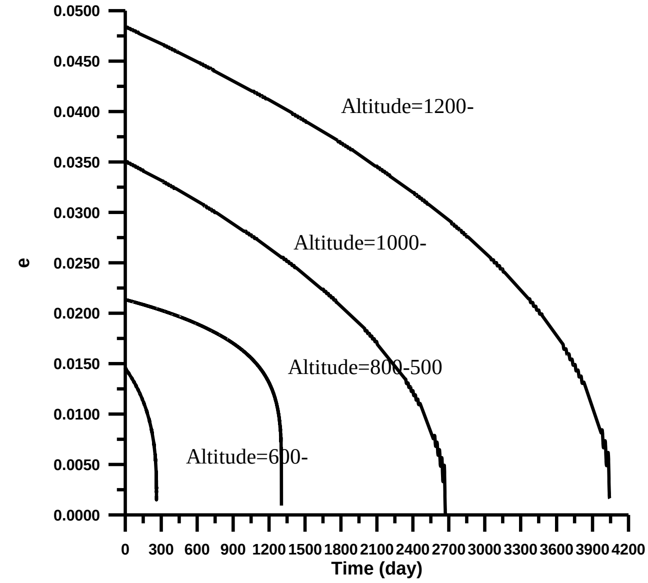

Fig.8: The behavior of eccentricity (e) with time of debris (diameter=1 cm).

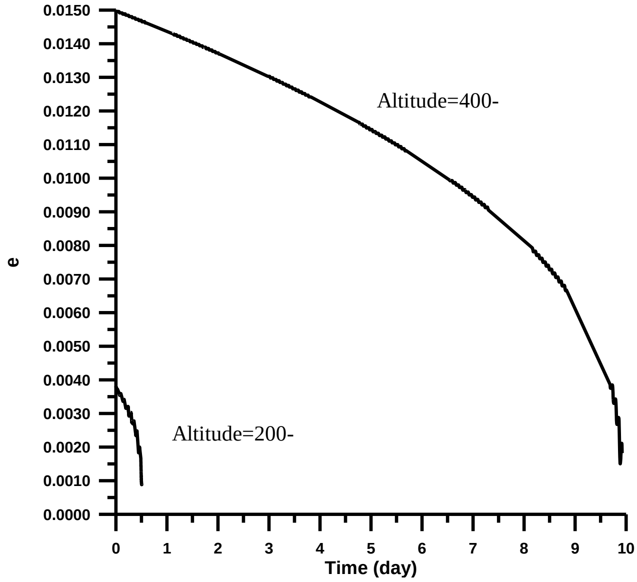

Fig.9: The behavior of eccentricity (e) with time of debris (diameter=1 cm).

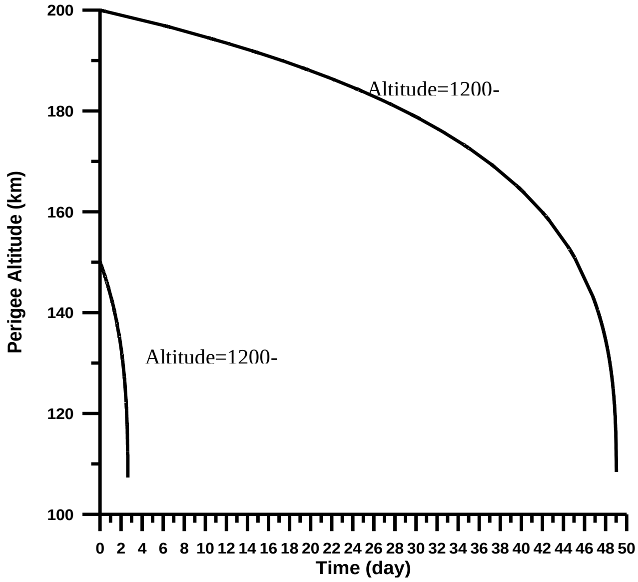

Fig.11: The behavior of height (hp) with time of debris (diameter=10 cm).

The apogee (ha) and perigee (hp) altitudes variations under atmospheric drag effects are shown in figures (10), (11), (12), (13) for (10 cm) diameters of space debris. The corresponding values of (1 cm) diameter space debris are shown in figures (14), (15), (16), (17). It can be estimated from these figures that the lifetime of the space debris depends on (1) apogee and perigee altitudes (2) area to mass ratio A/m.

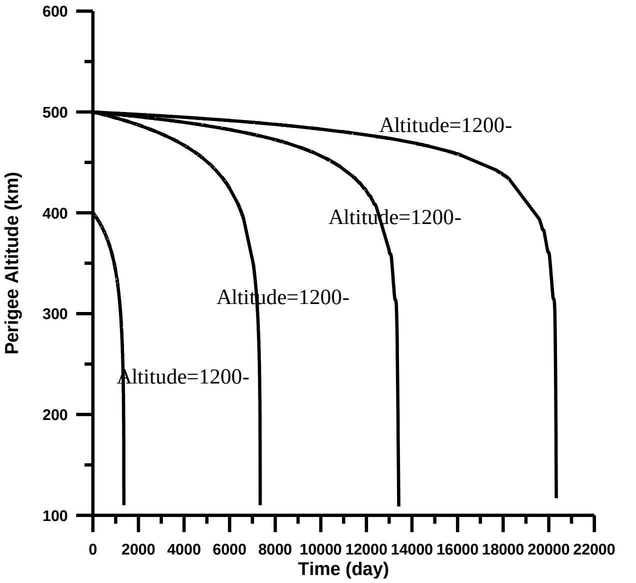

Fig.10: The behavior of height (hp) with time of debris (diameter=10 cm).

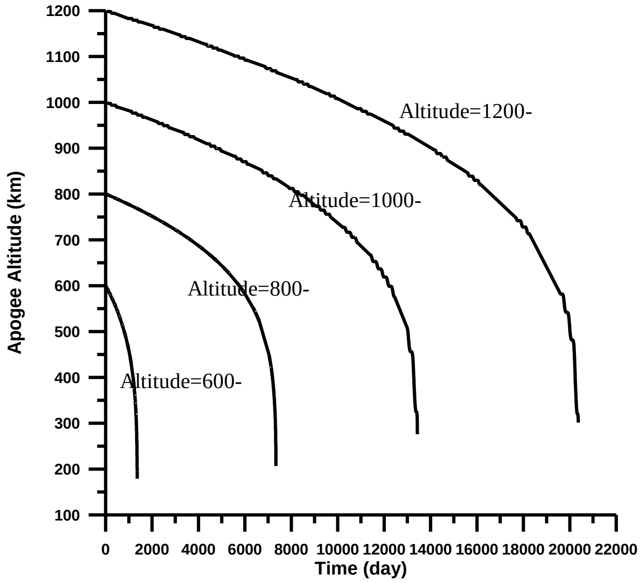

Fig.12: The behavior of height (hp) with time of debris (diameter=10 cm).

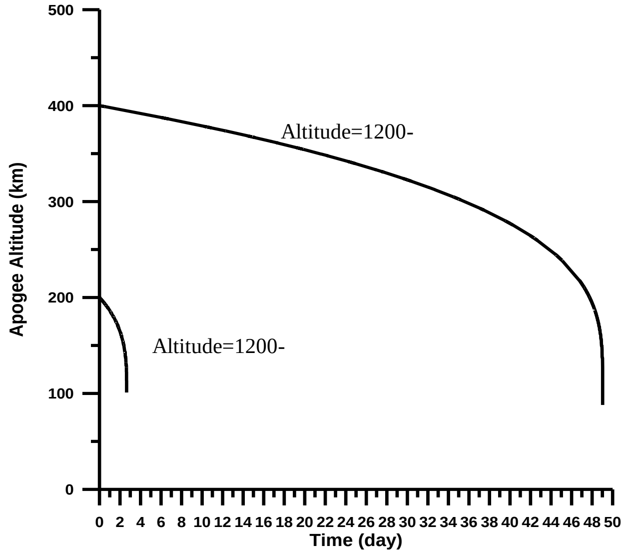

Fig.13: The behavior of height (hp) with time of debris (diameter=10 cm).

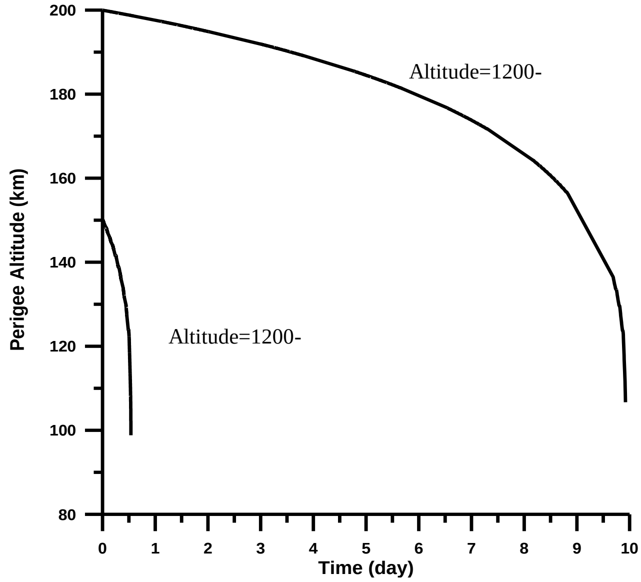

Fig.15: The behavior of height (hp) with time of debris (diameter=1 cm).

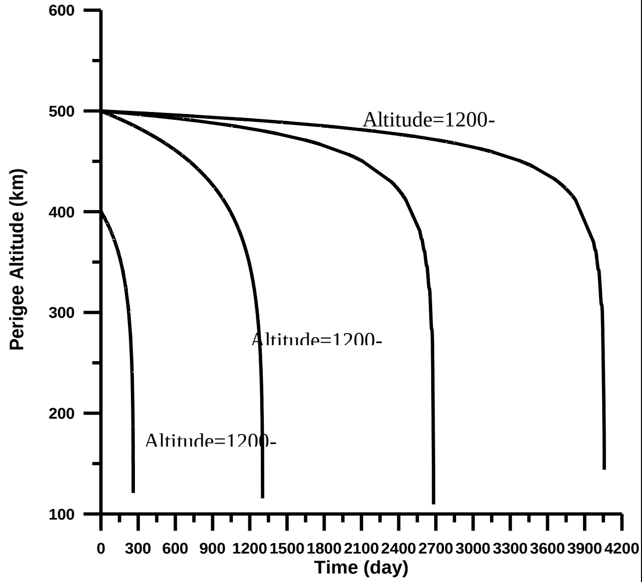

Fig.14: The behavior of height (hp) with time of debris (diameter=1 cm).

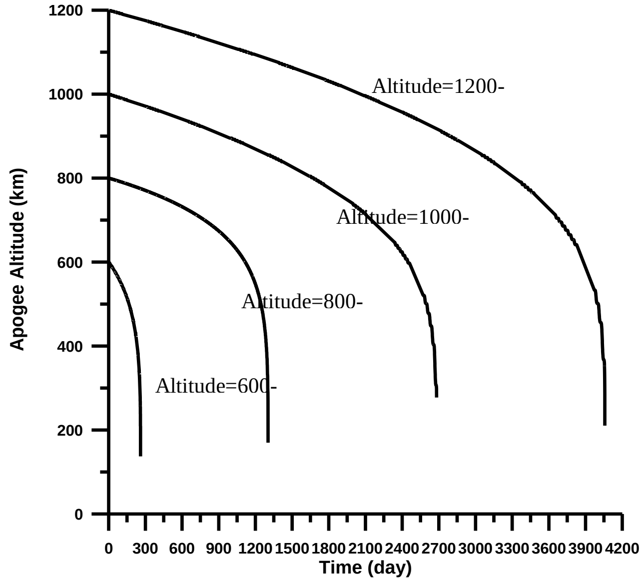

Fig.16: The behavior of height (ha) with time of debris (diameter=1 cm).

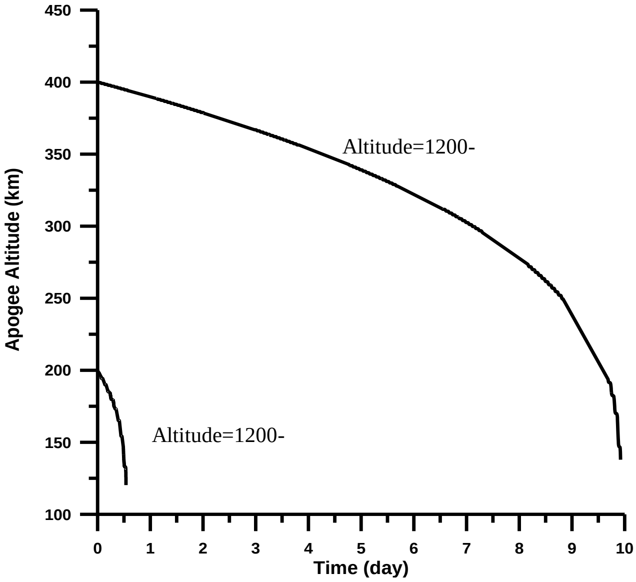

Fig.17: The behavior of height (ha) with time of debris (diameter=1 cm).

1. Conclusions

This work focuses on simulation of orbital dynamics of space debris of size range (1and 10 cm) of aluminum type and their reentry dynamics from the apogee-perigee altitudes 1200 to 200 km. This work is distinguished by the selection of aluminum in specific sizes with different altitudes. The lifetime of the debris in its orbit under the effects of gravitational force and atmospheric drag forces were evaluated. The lifetime depends on apogee and perigee altitudes. The longest lifetime is 55 years at altitudes (1200-500 km) with diameter (10 cm). The shortest lifetime is 3 days at altitudes (200-150 km) with diameter (10 cm). Similarly, the lifetime of space debris of (1 cm) diameter is estimated. The longest lifetime is 11 years and the corresponding shortest is 0.5 day. It has been found that lifetime depends on the area to mass ratio (A/m), apogee-perigee altitudes, the shape of the object (i.e. the drag coefficient C_d=2 for spherical object), the semi major axis, the eccentricity of the orbit and the atmospheric density of the upper atmosphere. The results can be used in any reentry space debris study such as reentry space debris by Laser.

5. REFERENCES

[1] A.E. Roy, "Orbital Motion", Adam Hilger Ltd, Bristol, New York, 1978.

[2] K.J. Ball, and G.F. Osborne, "Space Vehicle Dynamics", Oxford University Press, Ely House, London W.1, 1967.

[3] V.A. Chobotov, "Orbital mechanics", AIAA, second edition, 1996.

[4] W.I. Yaseen, "Trajectory analysis of reentry vehicles", M.Sc. thesis, Physics Department., College of Science, University of Baghdad, Iraq, 2001.

[5] C.R. Phipps, H. Friedman, D. Gavel, J.

[6] Murray, G. Albrecht, E. V. George, C. Ho, W. Priedhorsky, M. M. Michaelis, J. P. Reilly, "ORION: Clearing near-earth space debris using a 20-KW, 530-nm, Earth-based, repetitively pulsed laser", Laser and Particle Beams, 14(1) (1996) pp. 1-44.

[7] J.T. Early, C. Bibeau, C.R. Phipps, "Space debris de-orbiting by vaporization impulse using short pulse laser", AIP Conference Proceedings 702 (2004) 190.

[8] F.T. Geyling, H.R. Westerman, "Introduction to Orbital mechanics", Addison-Wesley Publishing Company, USA, 1971.

[9] R.M. Oubiad, "The Effect of Solar activity on the Orbits of Artificial Satellites of Low Altitude", M.Sc. Thesis, Babylon University, College of Science, Iraq, 2002.

[10] H. William, and S.A. Teukolsky, "Numerical Recipes in C: The Art of Scientific Computing ", Cambridge University Press, second edition, UK, 1992.

[11] R.H. Pennington, “Introductory Computer Methods and Numerical Analysis", The Macmillan Company Collier-MacmillanLTD.,London, 1970.

[12] C. Berger, R. Biancale, M. Ill, F. Barlier, "Improvement of the empirical thermospheric model DTM: DTM94 a comparative review of various temporal variations and prospects in space geodesy applications", Journal of Geodesy, 72 (1998)161-178,

[13] S. Shen, X. Jin, C. Hao: “Cleaning space debris with a space-based laser system”. Chinese Journal of Aeronautics, 27(4) (2014) 805–811.

[14] D. Hampf, W. Riede, G. Stockle, I. Buske: “Ground-based optical position measurements of space debris in low earth orbits”, Deutscher Luft-und Raumfahrtkongress, national Conference, Germany, 2013.